Mechanism and Dynamics of Translesion DNA Synthesis Catalyzed by the Escherichia coli Klenow Fragment †

ARTICLE *in* BIOCHEMISTRY · AUGUST 2008

Impact Factor: 3.02 · DOI: 10.1021/bi800324r · Source: PubMed

4 AUTHORS, INCLUDING:

Edward A Motea
University of Texas Southwestern Medical Ce…
15 PUBLICATIONS **91** CITATIONS
SEE PROFILE

Irene Lee
Case Western Reserve University
57 PUBLICATIONS **1,000** CITATIONS
SEE PROFILE

Anthony J Berdis
Cleveland State University
72 PUBLICATIONS **1,203** CITATIONS
SEE PROFILE

Published in final edited form as:
Biochemistry. 2008 August 19; 47(33): 8527–8537. doi:10.1021/bi800324r.

The Mechanism and Dynamics of Translesion DNA Synthesis Catalyzed by the *Escherichia coli* Klenow fragment

Asim Sheriff[a], **Edward Motea**[b], **Irene Lee**[b], and **Anthony J. Berdis**[a]

a*Department of Pharmacology, Case Western Reserve University, 10900 Euclid Avenue, Cleveland, Ohio 44106*

b*Department of Chemistry, Case Western Reserve University, 10900 Euclid Avenue, Cleveland, Ohio 44106*

Abstract

Translesion DNA synthesis represents the ability of a DNA polymerase to incorporate and extend beyond damaged DNA. In this report, the mechanism and dynamics by which the *Escherichia coli* Klenow fragment performs translesion DNA synthesis during the misreplication of an abasic site were investigated using a series of natural and non-natural nucleotides. Like most other high fidelity DNA polymerases, the Klenow fragment follows the "A-rule" of translesion DNA synthesis by preferentially incorporating dATP opposite the non-instructional lesion. However, several 5-substituted indolyl nucleotides lacking classical hydrogen-bonding groups are incorporated ~100-fold more efficiently than the natural nucleotide. In general, analogs that contain large substituent groups in conjunction with significant π-electron density display the highest catalytic efficiencies (k_{cat}/K_m) forincorporation. While the measured K_m values depend upon the size and π-electron density of the incoming nucleotide, k_{cat} values are surprisingly independent of both biophysical features. As expected, the efficiency by which these non-natural nucleotides are incorporated opposite templating nucleobases is significantly reduced. This reduction reflects minimal increases in K_m values coupled with large decreases in k_{cat}. The kinetic data obtained with the Klenow fragment are compared to that of the high fidelity bacteriophage T4 DNA polymerase and reveal distinct differences in the dynamics by which these non-natural nucleotides are incorporated opposite an abasic site. These biophysical differences argue against a unified mechanism of translesion DNA synthesis and suggest that polymerases employ different catalytic strategies during the misreplication of damaged DNA.

Keywords

DNA polymerization; base-stacking; desolvation; π-electrons; catalysis

DNA polymerases catalyze the addition of dNTPs into a growing polymer (primer) using a DNA template as a guide for directing each incorporation event. Although the chemical mechanism of this phosphoryl transfer reaction is well-defined (1), several questions remain as to how most DNA polymerases maintain an incredible degree of substrate fidelity during this reaction. Maintaining fidelity during DNA replication is a daunting challenge since the changing nature of the heteropolymeric DNA template places strains on the unusually high demand for substrate specificity. Replication fidelity has historically been interpreted with respect to the formation of proper hydrogen bonds between the nascent base pairs (2-5). In this model, the incoming dNTP directly pairs opposite its complementary template partner via direct hydrogen bonding and the enzyme catalyzes phosphodiester bond formation only if the

Corresponding Author Information: Telephone (216)-368-4723, Fax (216) 368-3395, e-mail: E-mail: ajb15@case.edu.

two nucleobases align correctly. As such, misincorporation events rarely occur since ground-state dNTP binding and/or the chemical rate become significantly worse if the functional groups present on both nucleotides do not align properly. While elegantly simple, this model appears incomplete since the frequency of misincorporation events are typically lower than what is predicted from the free energy differences (ΔΔG°) between matched and mismatched base pairs (reviewed in 6 and 7).

To reconcile this dichotomy, several model systems have been used to evaluate the role of hydrogen bonding interactions during polymerization (8-11). One powerful approach is the use of non-natural nucleotides containing diverse functional groups such as -F, -Cl, and -NO_2 that are not considered classical hydrogen bonding groups (10-15). Several laboratories have shown that various non-natural nucleotides are incorporated opposite templating nucleobases with surprisingly high catalytic efficiencies (10-15). These data suggest that the predominant force in optimizing polymerization is the proper geometrical alignment of the incoming nucleotide with its templating partner rather than hydrogen bonding interactions. However, a pitfall of this approach is that removing or altering a functional group of the incoming nucleotide also inadvertently influences additional biophysical parameters including the tautomeric form, aromaticity, and solvation energies of the nucleotide. Since each of these biophysical features contribute to polymerization efficiency, developing an accurate structure-activity relationship becomes exceedingly complex.

Another useful approach to evaluate the role of hydrogen-bonding interactions and steric constraints is to monitor nucleotide incorporation opposite damaged DNA. In this present study, we evaluate the ability of the Klenow fragment from *Escherichia coli* to incorporate the series of natural and non-natural nucleotides opposite an abasic site (Figure 1). The advantage of using an abasic site is that the non-instructional lesion is devoid of hydrogen bonding interactions and size constraints imposed by a templating nucleobase. In addition, the library of 5-substituted indolyl nucleotides used in this study vary with respect to shape/size, solvation energies, dipole moment, and π-electron density. Thus, defining the kinetic parameters for their incorporation opposite this DNA lesion can generate a useful structure-activity relationship to accurately define which biophysical parameters influence the dynamics of translesion DNA synthesis. For example, our kinetic studies with the bacteriophage T4 DNA polymerase reveal that the efficiency of translesion DNA synthesis is governed predominantly by the π-electron and desolvation energies of the incoming nucleotide rather than its shape, size, and/or hydrogen-bonding potential (16-21).

This report evaluates whether or not this mechanism is universal amongst all DNA polymerases. It is known that the Klenow fragment preferentially incorporates dATP opposite the abasic site and thus follows the “A-rule” of translesion DNA synthesis (22-24) as does the bacteriophage T4 DNA polymerase (25). At face value, this similarity implies that the mechanism of translesion DNA synthesis is identical and governed by thermodynamic control, i.e., the intrinsic base-stacking properties of the incoming nucleotide. However, we report distinct differences in the kinetic parameters for the various 5-substituted indolyl nucleotides that reveal nuances in the dynamics of translesion DNA synthesis. These differences indicate that the dynamics of translesion DNA synthesis are under kinetic rather than thermodynamic control. Structural models based upon variations in the amino acid composition and architecture of the active site of each DNA polymerase are provided to explain the differences in kinetic behavior during translesion DNA synthesis.

MATERIALS AND METHODS

Materials

[γ-^{32}P] ATP was purchased from MP Biomedical (Irvine, CA). Unlabelled dNTPs (ultrapure) were obtained from Pharmacia. $MgCl_2$ and Trizma base were from Sigma. Urea, acrylamide, and bis-acrylamide were from Aldrich. Oligonucleotides, including those containing a tetrahydrofuran moiety mimicking an abasic site, were synthesized by Operon Technologies (Alameda, CA). dATP, dCTP, dGTP, and dTTP were obtained from Sigma in greater than 99% purity. All non-natural indolyl-deoxyribose triphosphates were synthesized, purified, and characterized as previously described (16-21). All other materials were obtained from commercial sources and were of the highest available quality. The Klenow fragment of *E. coli* DNA polymerase I was purified and quantified as previously described (26).

General Methods

5'-ends of the primer and template strands were labelled using [γ-^{32}P]-ATP and T4 polynucleotide kinase (GibcoBRL). Single-stranded and duplex DNA were purified and quantified as previously described (27). The assay buffer used in all kinetic studies consisted of 25 mM Tris-acetate (pH 7.5), 150 mM potassium acetate, and 10 mM 2-mercaptoethanol. All assays were performed at 25°C. Polymerization reactions were monitored by analysis of the products on 20% sequencing gels as described by Mizrahi *et al* (28). Gel images were obtained with a Packard PhosphorImager using the OptiQuant software supplied by the manufacturer. Product formation was quantified by measuring the ratio of ^{32}P-labelled extended and non-extended primer. The ratios of product formation are corrected for substrate in the absence of polymerase (zero point). Corrected ratios are then multiplied by the concentration of primer/template used in each assay to yield total product. All concentrations are listed as final solution concentrations.

Determination of the Kinetic Parameters for Nucleotide Incorporation

The kinetic parameters k_{cat}, K_m, and k_{cat}/K_m for natural and non-natural nucleotides during DNA synthesis were obtained by monitoring the rate of product formation using a fixed amount of Klenow fragment (12 or 60 nM) and DNA substrate (1 μM) at varying concentrations of nucleotide (10 - 500 μM). Aliquots of the reaction were quenched into 200 mM EDTA, pH 7.4 at times ranging from 5- 240 sec. Steady-state rates were obtained from the linear portion of the time course and were fit to equation 1

$$\text{rate}=mt+b \qquad \text{(eqn 1)}$$

where m is the slope of the line, b is the y-intercept, and t is time. The slope of the line is the rate of the polymerization reaction (nM/sec). Data for the dependency of rate as a function of nucleotide concentration were fit to the Michaelis-Menten equation (equation 2)

$$v=V_{max}[\text{dXTP}]/K_m+[\text{dXTP}] \qquad \text{(eqn 2)}$$

where v is the rate of product formation (nM/sec), V_{max} is the maximal rate of polymerization, K_m is the Michaelis constant for dXTP, and dXTP is the concentration of nucleotide substrate. The turnover number, k_{cat}, was obtained by dividing V_{max} by the concentration of Klenow fragment used in each experiment.

Pre-Steady State Nucleotide Incorporation Assays

To evidence for a two-step reaction mechanism, time courses were generated using a rapid quench instrument as previously described (29) to monitor for a "burst" in product formation. These experiments were performed mixing a preincubated solution of 100 nM Klenow fragment and 1 μM DNA with 100 μM EDTA against 500 μM nucleotide and 10 mM Mg^{2+} at time intervals ranging from 0.005 to 10 sec. The reactions were quenched through the addition of 350 mM EDTA. Quenched samples were diluted 1:1 with sequencing gel load buffer and products were analyzed for product formation by denaturing gel electrophoresis as described above.

Single Turnover Assays

These experiments were performed mixing a preincubated solution of 500 nM Klenow fragment and 200 nM DNA with 100 μM EDTA against 10 μM nucleotide and 10 mM Mg^{2+} at time intervals ranging from 5 to 300 sec. The reactions were quenched through the addition of 350 mM EDTA. Quenched samples were diluted 1:1 with sequencing gel load buffer and products were analyzed for product formation by denaturing gel electrophoresis as described above. Data obtained for single turnover rates in DNA polymerization were fit to equation 3:

$$y=A\left(1-e^{-kobs^{*}t}\right)+C \qquad \text{(eqn 3)}$$

where A is burst amplitude, k_{obs} is the first order rate constant, t is time, and C is a defined constant.

RESULTS AND DISCUSSION

Incorporation of Natural Nucleotides Opposite an Abasic Site

The dynamics of translesion DNA synthesis catalyzed by the *E. coli* Klenow fragment was first investigated by monitoring the incorporation of all four natural dNTPs opposite the non-instructional abasic site. The DNA sequence used in this study (Figure 1B) is identical to that previously employed in our studies using the bacteriophage T4 DNA polymerase (16-21, 25) so that valid mechanistic comparisons between the two DNA polymerases could be made. For example, the utilization of identical reaction conditions and DNA substrate allows us to evaluate if nucleotide incorporation is influenced by simple thermodynamic control versus a more complex mechanism involving kinetic control. If translesion DNA synthesis is under thermodynamic control, then nucleotide utilization should be dominated by the biophysical features of the nucleotide and be relatively independent of the DNA polymerase being assayed, i.e., dATP should be preferentially incorporated by both the Klenow fragment and T4 DNA polymerase. Representative gel electrophoresis provided in Figure 2A reveals that the Klenow fragment does indeed preferentially incorporate dATP opposite the abasic site while the other three natural nucleotides, dGTP, dCTP, and dTTP, are poorly incorporated. These results are nearly identical to the bacteriophage T4 DNA polymerase in which the purines dATP and dGTP are incorporated ~10-fold more efficiently than the pyrimidines, dCTP and dTTP (25). At face value, the similar preference for nucleotide incorporation opposite an abasic site suggests that the dynamics of translesion DNA replication lesion are identical between the distinct DNA polymerases and argue for a mechanism involving thermodynamic control for the nucleotide incorporation.

To further evaluate this hypothesis, the kinetic parameters, K_m, k_{cat}, and k_{cat}/K_m, were measured for dATP incorporation opposite the abasic site. Rates for nucleotide incorporation were monitored varying the concentration of dATP from 10 to 500 μM while maintaining the

concentration of Klenow fragment and abasic site-containing DNA fixed at 12 nM and 1 μM, respectively. Representative data provided in Figure 2B illustrates the dependency on the rate in primer elongation as a function of dATP concentration. Each time course in primer elongation is linear under the time frame tested and were fit to equation 1 to obtain initial rates. The plot of rate versus dATP concentration is hyperbolic (Figure 2C) and a fit to the Michaelis-Menten equation yields a K_m of 146 +/- 46 μM, a k_{cat} of 0.8 +/- 0.1 sec^{-1}, and a k_{cat}/K_m of 5,500 M^{-1} sec^{-1}. Kinetic parameters for the other natural nucleotides could not be accurately measured as the amount of product formation was less than 5% even at high concentrations of dNTP tested (500 μM).

While dATP is preferentially utilized by both the Klenow fragment and T4 DNA polymerase, these enzymes differ significantly with respect to their kinetic parameters. For example, the T4 DNA polymerase appears to bind dATP with higher affinity as manifest in a 4-fold lower K_m for dATP (compare 35 μM versus 145 μM, respectively).[2] However, the Klenow fragment has a 5-fold faster rate constant for dATP incorporation compared to the T4 DNA polymerase (compare k_{cat} values of 0.8 sec^{-1} versus 0.15 sec^{-1}, respectively) (25).[3] In general, these differences argue that the dynamics of translesion DNA synthesis catalyzed by these polymerases are not identical as presumed. Thus, the preferential utilization of nucleotides opposite a non-instructional DNA lesion may be governed by kinetic rather than thermodynamic control.

Incorporation of Non-Natural Nucleotides Opposite an Abasic Site

We next assessed the ability of the *E. coli* Klenow fragment to incorporate the series of 5-substituted indolyl-deoxyriboside triphosphates opposite an abasic site to further define differences in dynamics of translesion DNA synthesis. Representative gel electrophoresis data provide in Figure 3A illustrates that certain non-natural nucleotides are incorporated opposite this lesion with relatively high efficiencies. In general, large nucleotides such as 5-CH-ITP and 5-NapITP are incorporated opposite the non-instructional lesion much more effectively than smaller nucleotides such as 5-FITP and 5-AITP.

To further quantify these differences, K_m and k_{cat} values were measured as described above. Representative data provided in Figure 3B illustrates the dependency on the rate of primer elongation as a function of 5-NITP concentration. The plot of rate versus 5-NITP concentration is again hyperbolic (Figure 3C) and a fit of the data to the Michaelis-Menten equation yields a K_m of 74 +/- 14 μM, a k_{cat} of 2.3 +/- 0.2 sec^{-1}, and a k_{cat}/K_m of 31,000 +/- 2,500 $M^{-1}sec^{-1}$.

Identical analyses were performed for the other 5-substituted indole triphosphates. Their K_m and k_{cat} values, summarized in Table 1, provide a useful structure-activity relationship highlighting the importance of various biophysical parameters toward efficient incorporation opposite the lesion. In general, the presence of π-electron density as well as the shape and size of the nucleobase are essential for efficient incorporation opposite the lesion. For example, large bulky analogs that contain π-electron density (5-CE-ITP, 5-PhITP, and 5-NapITP) are

[2]It should be noted that K_m values do not always provide accurate information regarding the binding affinity of a substrate. However, the K_m value can equal (or at least approximate) a true dissociation constant under conditions in which phosphoryl transfer or a kinetic step preceding phosphoryl transfer (conformational change) is the slowest step along the polymerization pathway. While previously published (29) and current data (vida infra) suggest that the conformational change is likely the rate-limiting step for nucleotide incorporation opposite an abasic site, we acknowledge that this is not unambiguous proof that this condition is met using our series of non-natural nucleotides.

[3]During correct DNA synthesis, the k_{cat} value typically reflects the release of polymerase from product DNA (30). This is unlikely for the incorporation of non-natural nucleotides opposite an abasic site for several reasons. First, time courses in nucleotide incorporation are linear and do not show a burst in primer elongation that would indicate a two step reaction mechanism (Supplemental Information 1). Furthermore, the rate constant for nucleotide incorporation measured under single turnover conditions is identical, within error, to the k_{cat} value measured using steady-state conditions (Supplemental Information 2). These two pieces of evidence suggest that the k_{cat} value reflects either the phosphoryl transfer step or, more likely, the conformational change step preceding phosphoryl transfer.

incorporated with high catalytic efficiencies of $>10^5$ M^{-1} sec^{-1}. Removal of π-electron density reduces the efficiency of nucleotide incorporation since the overall catalytic efficiency for 5-CH-ITP is 10-fold lower compared to analogs such as 5-CE-ITP and 5-PhITP that are similar in shape and size yet that contain π-electron density. However, nucleobase size also plays an important role since the catalytic efficiency for a small analog containing π-electron density such as 5-NITP is 10-fold lower than 5-CE-ITP and 5-PhITP. Finally, smaller analogs such as IndTP, 5-FITP, and 5-AITP that lack significant π-electron density are not incorporated opposite the non-instructional DNA lesion.

A more thorough analysis of the kinetic data reveals that k_{cat} values are relatively independent of the size of the non-natural nucleotide. Specifically, 5-NITP and 5-PhITP have identical k_{cat} values of ~2.4 sec^{-1} although they differ significantly with respect to both shape and size. Surprisingly, the measured k_{cat} values also appear independent of π-electron density since the value for 5-CH-ITP is essentially identical to that for 5-CE-ITP and 5-PhITP. One possibility is that the rate constant for incorporation is influenced by a combination of π-electron density and/or size of the incoming nucleotide coupled with its relative hydrophobicity since each analog has low solvation energies of <7.2 kcal/mol (refer to Table 1). The potential role of these biophysical features is described later within the context of the proposed structural models (vide infra).

In contrast to the rate constants for incorporation, K_m values for the non-natural nucleotides are highly dependent upon their π-electron surface areas. Analogs such as 5-NapITP, 5-PhITP, and 5-CE-ITP have very low K_m values of ~10 μM. The five-fold higher K_m value for 5-CH-ITP compared to 5-CE-ITP suggests that removal of π-electron density affects binding affinity. In addition, the K_m value for 5-NITP is ~12-fold lower than that for 5-CE-ITP despite the fact that both analogs have similar π-electron surface areas of ~180 $Å^2$. This suggests that the overall size of the incoming nucleotide also influences its binding affinity.

Incorporation of Non-Natural Nucleotides Opposite a Templating Thymine

To compare and contrast the dynamics of translesion versus normal DNA synthesis, we next measured the ability of the Klenow fragment to incorporate non-natural nucleotides opposite a templating thymine. The kinetic parameters, K_m, k_{cat}, and k_{cat}/K_m, were measured as previously described and are summarized in Table 2. In all cases, there is a marked reduction in the overall catalytic efficiency for incorporation opposite thymine as compared to an abasic site. One dramatic example is the low catalytic efficiency of 180 $M^{-1}sec^{-1}$ for 5-NITP incorporation opposite thymine. This value is ~170-fold lower than that measured during translesion DNA synthesis. Surprisingly, this reduction is caused by a small 2.5-fold decrease in the K_m value for 5-NITP coupled with a more significant 70-fold reduction in the k_{cat} value. In addition, it should be noted that 5-FITP is incorporated opposite thymine with a slightly higher overall catalytic efficiency of 400 $M^{-1}sec^{-1}$. This result is reminiscent of the facile incorporation of 2,4-difluorotoulene opposite a templating adenine (10) and indicates that DNA polymerization can occur even in the absence of classical hydrogen-bonding interactions between a natural and non-natural nucleobase (10-15). The ability of the polymerase to form these non-natural base pairs is often attributed to steric fit and shape complementarity.

While shape complementarity plays an important role during DNA polymerization, other biophysical features must also participate during this process. This is apparent for two reasons. First, the Klenow fragment does not incorporate non-natural nucleotides such as IndTP and 5-AITP opposite thymine even though they are arguably considered good mimetics of dATP (Supplemental Figure 3). Based upon the shape and size of these indolyl nucleotides, it was predicted that they would be efficiently inserted opposite thymine due to the expected favorable contributions of steric fit and, in the case of 5-AITP, potential hydrogen-bonding interactions of the amino group with the keto oxygen of thymine. The second argument is that large

nucleotides such as 5-PhITP and 5-NapITP are incorporated surprisingly well opposite thymine. Indeed, it is remarkable that the overall catalytic efficiencies for these non-natural nucleotides are equal or *higher* than those measured with smaller analogs such as 5-FITP. In fact, the catalytic efficiencies are related to the base-stacking potential of the non-natural nucleotide rather than its size, shape, and/or hydrogen bonding potential. In all cases, the most influential kinetic parameter is the K_m value which displays a unique correlation with the π-electron surface area of the incoming nucleotide. The k_{cat} values remain invariant as a function of π-electron density, a feature that is similar to what was observed during translesion DNA synthesis.

Is There a Unified Mechanism for Translesion DNA Synthesis?

It is established that most DNA polymerases follow the "A-rule" of translesion DNA synthesis as dATP is preferentially incorporated opposite an abasic site (22,25,31-33). The Klenow fragment and the bacteriophage T4 DNA polymerase are no exceptions as the catalytic efficiency for dATP incorporation is at least 10-fold greater than any other natural nucleotide. This result suggests that the mechanism and dynamics of translesion DNA are identical between these polymerases and implies that translesion DNA synthesis is governed by thermodynamic control. However, subtle differences in the kinetic parameters for dATP incorporation argue otherwise. Specifically, the Klenow fragment binds dATP with 4-fold lower affinity than the T4 polymerase while the maximal rate constant for dATP incorporation is 5-fold faster with Klenow fragment compared to the bacteriophage counterpart (vide infra).

A more complete picture is unveiled from the comprehensive analyses monitoring the incorporation of non-natural nucleotides opposite the abasic site. A critical comparison of the kinetic parameters provided in Table 3 reveal significant differences in the structure-activity relationship between the DNA polymerases.[4] In the case of the Klenow fragment, the K_m values of these non-natural nucleotides differ with respect to the presence of π-electron density on the incoming nucleotide. For example, the K_m of a non-natural nucleotide gradually decreases from a value of 34 μM with 5-CH-ITP to 6.3 μM with 5-CE-ITP. The increase in apparent binding affinity coincides with an increase in the π-electron surface area of the non-natural nucleotide. A contrasting mechanism is observed with the bacteriophage T4 DNA polymerase as K_d values for these particular non-natural nucleotides are relatively independent of π-electron surface areas.

In contrast to K_m, the k_{cat} values for analogs such as 5-CH-ITP, 5-CE-ITP, and 5-PhITP remain essentially invariant at ~2.6 sec^{-1}. As before, a different scenario is observed with the T4 polymerase as the maximal rate constant for nucleotide incorporation is sensitive to the presence of π-electron density (16-21). This is most evident by comparing the k_{pol} values of 0.4 sec^{-1} and 25 sec^{-1} measured with the bacteriophage polymerase for 5-CH-ITP and 5-CE-ITP, respectively (19). The slower k_{pol} value for 5-CH-ITP is attributed to the lack of π-electron density whereas the presence of π-electron density by virtue of a double bond in 5-CE-ITP gives rise to a 60-fold increase in k_{pol}.

If the dynamics of translesion DNA synthesis are under kinetic control, then the observed variations in kinetic behavior between the two DNA polymerases should be resolved by structural differences between the two enzymes. At face value, this seems unlikely since all structurally characterized DNA polymerases share a similar overall molecular architecture resembling a "right hand" containing fingers, palm, and thumb subdomains (34). The fingers domain plays an important role in maintaining fidelity during nucleotide incorporation as this

[4]The analysis provided here only focuses on 5-NITP, 5-CH-ITP, 5-CE-ITP, 5-PhITP, and 5-NapITP as these nucleotides are utilized by both DNA polymerases. Our analysis does not include non-natural nucleotides such as 5-FITP and 5-AITP since these analogs are utilized by the T4 DNA polymerase but not by the Klenow fragment during translesion DNA synthesis.

region interacts with the incoming dNTP and the templating base. The thumb domain also plays dual roles by positioning duplex DNA for the incoming dNTP and aiding in the translocation of the polymerase to the next templating position. The palm is the most closely conserved structural feature amongst all DNA polymerases as it contains at least two carboxylates that function during the phosphoryl transfer step through coordination of two catalytically essential metal ions. Figure 4 compares the active sites of Klenow fragment (35-38) with the bacteriophage DNA polymerase (39-42) using the available ternary structures (polymerase:DNA:dNTP).[5] The catalytic aspartic acid residues (displayed in white) are nearly superimposable as they lie within ~4Å of the α-phosphate of the incoming nucleoside triphosphate (Figure 4 and insets). In addition, there is significant identity with respect to both the number and arrangement of positively charged amino acids (displayed in blue) that interact with the phosphate groups of the incoming dNTP. Both observations are consistent with the proposition that the chemical mechanism for phosphoryl transfer is universal amongst all DNA polymerases (44).

Despite the obvious similarities in these catalytic amino acids, there are distinct differences in the overall architecture of the polymerases' active sites. The global projections provided in Figure 4 reveal that the active site of the Klenow fragment is more densely populated compared to the active site of the bacteriophage DNA polymerase. The Klenow fragment has several large hydrophobic amino acids including Y671, F667, and L616 that are within 6Å of the primer-template junction. Although similar hydrophobic amino acids exist within the active site of the bacteriophage enzyme (Y567, F282, and L561), they lie in different orientations with respect to the primer-template. This is more evident in the models provided in Figure 5 which clearly show differences in the arrangements the two conserved aromatic amino acids with respect to the position of the incoming nucleotide. In the case of the Klenow fragment, these amino acids lie parallel to the incoming nucleobase and exist in position for optimal π-π stacking interactions. The same amino acids in the bacteriophage polymerase exist in a perpendicular configuration with the incoming nucleotide and could stabilize interactions through an offset π-π stacking arrangement (45).

The differences in amino acid composition and orientation suggest that the active site of the Klenow fragment is “tighter” compared to the active site of the bacteriophage polymerase. The difference in size could explain the variations in kinetic behavior for the incorporation of non-natural nucleotides opposite the abasic site. For example, the “tighter” active site of the Klenow fragment could explain why the dynamics of non-natural nucleotide incorporation depend more on the shape and size of the incoming nucleotide compared to the T4 DNA polymerase. This observation is consistent with the proposed steric fit model (46) since large, bulky analogs are preferentially incorporated opposite an abasic site as they occupy the same space as a normal Watson-Crick base pair. In fact, the facile incorporation of dPTP opposite an abasic site was taken as evidence for the contributions of steric fit and shape complementarity during translesion DNA synthesis (47). However, the pyrene analog also contains significant π-electron density that undoubtedly influences the kinetics of incorporation. Indeed, we demonstrate here that the Klenow fragment efficiently incorporates smaller nucleotide analogs such as 5-CE-ITP and 5-NITP that also contain conjugated double bonds. Our results coupled with those of the Kool laboratory (47) demonstrate that non-natural nucleotides containing π-

[5]A complete three-dimensional structure of the bacteriophage T4 DNA polymerase is currently unavailable. Thus, structures of the RB69 DNA polymerases (39-42) were used to provide insight into the mechanism and dynamics of translesion DNA replication. The high sequence identity (63%) and homology (92%) between the RB69 DNA polymerase and gp43 of bacteriophage T4 (43) implies a reasonable conservation in structure between the two enzymes. In addition, the structure for the ternary complex (polymerase:DNA:dNTP) of the KlenTaq DNA polymerase was used rather than the binary complexes of the *E. coli* Klenow fragment bound to DNA. This was necessary to evaluate differences between the ternary structures of either polymerase. This approach is valid since the active sites of KlenTaq and *E. coli* Klenow fragment are 84.8% identical and 95.3% homologous. In fact, an overlay of the two polymerases reveals that they are essentially identical in global and local structure (RMSD = 2.57789) (see Supplemental Information 4).

electron density are inserted ~100-fold more efficiently than any dNTP opposite the abasic site. Collectively, these results argue that the Klenow fragment utilizes a combination of size/shape and π-electron density during translesion DNA synthesis. This mechanism, illustrated in Figure 6, suggests that the large π-electron surface area of 5-phenylindole allows for more effective stacking interactions within the void of the DNA lesion compared to the smaller 5-nitroindole. This model suggests that the reduced stacking interactions of 5-nitroindole accounts for its higher K_m value compared to the larger 5-phenylindole moiety which has a ~25-fold lower Km value (compare 74 versus 2.8 μM, respectively).

In addition to variations in the "size" of either polymerase's active site, there are notable differences with respect to the number of hydrophilic and hydrophobic amino acids lining each active site that could also influence the dynamics of nucleotide incorporation. As illustrated in Figure 4, the active site of the Klenow fragment possesses a region of positively charged amino acids that could interact with the nucleobase portion of the incoming dNTP. In contrast, the active site of the phage polymerase is relatively more hydrophobic due to the presence of aromatic (displayed in yellow) and aliphatic (displayed in green) amino acids in the corresponding positions. This information suggests that the dynamics of nucleotide incorporation could also be influenced by differences in solvation energies associated with the various 5-substituted indolyl nucleotides.

We note that these models cannot be unambiguously used to determine which amino acid directly interacts with a defined functional group present on the incoming nucleobase. This deficiency likely reflects the complexity of the DNA polymerization reaction in which various physical (nucleotide binding, conformational changes, etc.) and chemical (phosphoryl transfer) steps occur during this process. It is likely that the coordination of these physical and chemical steps requires the balanced efforts of numerous amino acids within the enzyme's active site. In addition, many of these amino acids possess diverse properties that could perform different functions during the polymerization cycle. Amino acids such as tyrosine and phenylalanine are exceptionally versatile as their aromatic nature allows them to provide π-π and π-cation stacking interactions while their aliphatic nature provides opportunities to participate in the desolvation of the incoming nucleotide as it enters the hydrophobic interior of the DNA helix. In this respect, it is interesting that mutagenesis studies of Y766 in Klenow fragment (Y761 in the Klentaq structures) reveal an important role for this amino acid in the kinetics and fidelity of polymerization (48-50). Early work in the Benkovic laboratory showed that the catalytic efficiency for correct nucleotide incorporation by the Y766S is five-fold lower than the wild-type polymerase (48). However, the Y766S mutant also displayed reduced fidelity as it displayed an increased efficiency for dNTP misincorporation opposite a non-complementarity partner (48). Surprisingly, there was not a global reduction in fidelity as the formation of certain mismatches (dTMP misincorporation opposite guanine) occurs more efficiently compared to other mismatches such as the misincorporation of dAMP opposite template A, G, or C (48). Similar findings have been reported by the Kunkel and Joyce laboratories (49) and re-iterate the importance of this amino acid during the proper replication of un-damaged DNA.

There are no reports regarding the influence of this amino acid on the misreplication of an abasic site. However, a recent report from the Romano laboratory showed that the Y766S mutant incorporates nucleotides opposite N-acetyl-2-aminofluorene more efficiently than the wild-type polymerase (50). This rate enhancement is caused by the ability of the Y766S mutant to undergo the conformational change when bound to the bulky carcinogenic adduct whereas the wild-type enzyme can not (50). This result again suggests that the tyrosine residue can play diverse roles in base-stacking, desolvation, and size constraints during the polymerization cycle. We are currently evaluating the role of Y766 and other aromatic amino acids in the misreplication of an abasic site to further define its role in translesion DNA synthesis.

Supplementary Material

Refer to Web version on PubMed Central for supplementary material.

Acknowledgment

We would like to dedicate this manuscript to Professor Stephen J. Benkovic and Patricia Benkovic in honor of their 70^{th} birthdays and to commemorate their pioneering work in the field of DNA replication.

The research was supported through funding from the National Institutes of Health (CA118408) to AJB.

Abbreviations

TBE, Tris-HCl/borate/EDTA
EDTA, ethylenediaminetetraacetate, sodium salt
dNTP, 2-deoxynucleoside triphosphate
dXTP, , non-natural deoxynucleoside triphosphate
dATP, 2'-deoxyadenosine 5'-triphosphate
dCTP, 2'-deoxycytosine 5' triphosphate
dGTP, 2'-deoxyguanosine 5'-triphosphate
dTTP, 2'-deoxythymine 5'-triphosphate
5-FITP, 1-(2-deoxy-β-D-*erythro*-pentafuranosyl)-5-fluoroindole triphosphate
5-AITP, 1-(2-deoxy-β-D-*erythro*-pentafuranosyl)-5-aminoindole triphosphate
5-NITP, 1-(2-deoxy-β-D-*erythro*-pentafuranosyl)-5-nitroindole triphosphate
5-NapITP, 1-(2-deoxy-β-D-*erythro*-pentafuranosyl)-5-napthylindole triphosphate
5-PhITP, 1-(2-deoxy-β-D-*erythro*-pentafuranosyl)-5-phenylindole triphosphate
5-CE-ITP, 1-(2-deoxy-β-D-*erythro*-pentafuranosyl)-5-cyclohexenylindole triphosphate
5-CH-ITP, 1-(2-deoxy-β-D-*erythro*-pentafuranosyl)-5-cyclohexylindole triphosphate
dPTP, pyrene triphosphate

REFERENCES

1. Knowles JR. Enzyme-catalyzed phosphoryl transfer reactions. Annu. Rev. Biochem 1980;49:877–919. [PubMed: 6250450]
2. Kunkel TA, Bebenek K. DNA replication fidelity. Annu. Rev. Biochem 2000;69:497–529. [PubMed: 10966467]
3. Johnson KA. Conformational coupling in DNA polymerase fidelity. Annu. Rev. Biochem 1993;62:685–713. [PubMed: 7688945]
4. Goodman MF, Fygenson KD. DNA polymerase fidelity: from genetics toward a biochemical understanding. Genetics 1998;148:1475–1482. [PubMed: 9560367]
5. Beckman RA, Loeb LA. Multi-stage proofreading in DNA replication. Q. Rev. Biophys 1993;26:225–331. [PubMed: 8022969]
6. Loeb LA, Kunkel TA. Fidelity of DNA synthesis. Annu. Rev. Biochem 1982;51:429–457. [PubMed: 6214209]
7. Petruska J, Sowers LC, Goodman MF. Comparison of nucleotide interactions in water, proteins, and vacuum: model for DNA polymerase fidelity. Proc. Natl. Acad. Sci. U.S.A 1986;83:1559–1562. [PubMed: 3456600]
8. Horlacher J, Hottiger M, Podust VN, Hubscher U, Benner SA. Recognition by viral and cellular DNA polymerases of nucleosides bearing bases with nonstandard hydrogen bonding patterns. Proc. Natl. Acad. Sci. U.S.A 1995;92:6329–6933. [PubMed: 7541538]
9. Rappaport HP. The fidelity of replication of the three-base-pair set adenine/thymine, hypoxanthine/cytosine and 6-thiopurine/5-methyl-2-pyrimidinone with T7 DNA polymerase. Biochem. J 2004;381:709–717. [PubMed: 15078225]

10. Moran S, Ren RX, Kool ET. A thymidine triphosphate shape analog lacking Watson-Crick pairing ability is replicated with high sequence selectivity. Proc. Natl. Acad. Sci. U.S.A 1997;94:10506–10511. [PubMed: 9380669]
11. Morales JC, Kool ET. Efficient replication between non-hydrogen-bonded nucleoside shape analogs. Nat. Struct. Biol 1998;5:950–954. [PubMed: 9808038]
12. Tae EL, Wu Y, Xia G, Schultz PG, Romesberg FE. Efforts toward expansion of the genetic alphabet: replication of DNA with three base pairs. J. Am. Chem. Soc 2001;123:7439–7440. [PubMed: 11472182]
13. Paul N, Nashine VC, Hoops G, Zhang P, Zhou J, Bergstrom DE, Davisson VJ. DNA polymerase template interactions probed by degenerate isosteric nucleobase analogs. Chem. Biol 2003;10:815–825. [PubMed: 14522052]
14. Chiaramonte M, Moore CL, Kincaid K, Kuchta RD. Facile polymerization of dNTPs bearing unnatural base analogues by DNA polymerase alpha and Klenow fragment (DNA polymerase I). Biochemistry 2003;42:10472–10481. [PubMed: 12950174]
15. Hirao I, Fujiwara T, Kimoto M, Mitsui T, Okuni T, Ohtsuki T, Yokoyama S. Unnatural base pairs between 2-amino-6-(2-thienyl)purine and the complementary bases. Nucleic Acids Symp. Ser 2000;44:261–262. [PubMed: 12903368]
16. Reineks EZ, Berdis AJ. Evaluating the contribution of base stacking during translesion DNA replication. Biochemistry 2004;43:393–404. [PubMed: 14717593]
17. Zhang X, Lee I, Berdis AJ. Evaluating the contributions of desolvation and base-stacking during translesion DNA synthesis. Org. Biomol. Chem 2004;2:1703–1711. [PubMed: 15188037]
18. Zhang X, Lee I, Berdis AJ. The use of nonnatural nucleotides to probe the contributions of shape complementarity and pi-electron surface area during DNA polymerization. Biochemistry 2005;44:13101–13110. [PubMed: 16185078]
19. Zhang X, Lee I, Zhou X, Berdis AJ. Hydrophobicity, shape, and pi-electron contributions during translesion DNA synthesis. J. Am. Chem. Soc 2006;128:143–149. [PubMed: 16390141]
20. Devadoss B, Lee I, Berdis AJ. Enhancing the "A-rule" of translesion DNA synthesis: promutagenic DNA synthesis using modified nucleoside triphosphates. Biochemistry 2007;46:13752–13761. [PubMed: 17983244]
21. Vineyard D, Zhang X, Donnelly A, Lee I, Berdis AJ. Optimization of non-natural nucleotides for selective incorporation opposite damaged DNA. Org. Biomol. Chem 2007;5:3623–3630. [PubMed: 17971991]
22. Schaaper RM, Kunkel TA, Loeb LA. Infidelity of DNA synthesis associated with bypass of apurinic sites. Proc. Natl. Acad. Sci. U.S.A 1983;80:487–491. [PubMed: 6300848]
23. Boiteux S, Laval J. Coding properties of poly(deoxycytidylic acid) templates containing uracil or apyrimidinic sites: in vitro modulation of mutagenesis by deoxyribonucleic acid repair enzymes. Biochemistry 1982;21:6746–6751. [PubMed: 6760893]
24. Efrati E, Tocco G, Eritja R, Wilson SH, Goodman MF. Abasic translesion synthesis by DNA polymerase beta violates the "A-rule". Novel types of nucleotide incorporation by human DNA polymerase beta at an abasic lesion in different sequence contexts. J. Biol. Chem 1997;272:2559–2569. [PubMed: 8999973]
25. Berdis AJ. Dynamics of translesion DNA synthesis catalyzed by the bacteriophage T4 exonuclease-deficient DNA polymerase. Biochemistry 2001;40:7180–7191. [PubMed: 11401565]
26. Joyce CM, Derbyshire V. Purification of *Escherichia coli* DNA polymerase I and Klenow fragment. Methods Enzymol 1995;262:3–13. [PubMed: 8594356]
27. Capson TL, Peliska JA, Kaboord BF, Frey MW, Lively C, Dahlberg M, Benkovic SJ. Kinetic characterization of the polymerase and exonuclease activities of the gene 43 protein of bacteriophage T4. Biochemistry 1992;31:10984–10994. [PubMed: 1332748]
28. Mizrahi V, Benkovic PA, Benkovic SJ. Mechanism of DNA polymerase I: exonuclease/polymerase activity switch and DNA sequence dependence of pyrophosphorolysis and misincorporation reactions. Proc. Natl. Acad. Sci. U.S.A 1986;83:5769–5773. [PubMed: 3016719]
29. Lee I, Berdis A. Fluorescent analysis of translesion DNA synthesis by using a novel, non-natural nucleotide analogue. ChemBioChem 2006;7:1990–1997. [PubMed: 17091513]

30. Kuchta RD, Mizrahi V, Benkovic PA, Johnson KA, Benkovic SJ. Kinetic mechanism of DNA polymerase I (Klenow). Biochemistry 1987;26:8410–8417. [PubMed: 3327522]
31. Shibutani S, Takeshita M, Grollman AP. Translesional synthesis on DNA templates containing a single abasic site. A mechanistic study of the "A rule". J. Biol. Chem 1997;27:13916–13922. [PubMed: 9153253]
32. Paz-Elizur T, Takeshita M, Livneh Z. Mechanism of bypass synthesis through an abasic site analog by DNA polymerase I. Biochemistry 1997;36:1766–1773. [PubMed: 9048560]
33. Strauss BS. The 'A rule' of mutagen specificity: a consequence of DNA polymerase bypass of non-instructional lesions? Bioessays 1991;13:79–84. [PubMed: 2029269]
34. Steitz TA. DNA polymerases: Structural diversity and common mechanisms. J. Biol. Chem 1999;274:17395–17398. [PubMed: 10364165]
35. Yadav PN, Yadav JS, Modak MJ. A molecular model of the complete three-dimensional structure of the Klenow fragment of *Escherichia coli* DNA polymerase I: binding of the dNTP substrate and template-primer. Biochemistry 1992;31:2879–2886. [PubMed: 1550814]
36. Beese LS, Derbyshire V, Steitz TA. Structure of DNA polymerase I Klenow fragment bound to duplex DNA. Science 1993;260:352–355. [PubMed: 8469987]
37. Beese LS, Friedman JM, Steitz TA. Crystal structures of the Klenow fragment of DNA polymerase I complexed with deoxynucleoside triphosphate and pyrophosphate. Biochemistry 1993;32:14095–14101. [PubMed: 8260491]
38. Li Y, Korolev S, Waksman G. Crystal structures of open and closed forms of binary and ternary complexes of the large fragment of *Thermus aquaticus* DNA polymerase I: structural basis for nucleotide incorporation. EMBO J 1998;17:7514–7525. [PubMed: 9857206]
39. Franklin MC, Wang J, Steitz TA. Structure of the replicating complex of a pol alpha family DNA polymerase. Cell 2001;105:657–667. [PubMed: 11389835]
40. Hogg M, Wallace SS, Doublie S. Crystallographic snapshots of a replicative DNA polymerase encountering an abasic site. EMBO J 2004;23:1483–1493. [PubMed: 15057283]
41. Freisinger E, Grollman AP, Miller H, Kisker C. Lesion (in)tolerance reveals insights into DNA replication fidelity. EMBO J 2004;23:1494–505. [PubMed: 15057282]
42. Zahn KE, Belrhali H, Wallace SS, Doublié S. Caught bending the A-rule: crystal structures of translesion DNA synthesis with a non-natural nucleotide. Biochemistry 2007;18:10551–10561. [PubMed: 17718515]
43. Karam JD, Konigsberg WH. DNA polymerase of the T4-related bacteriophages. Prog. Nucleic Acid Res. Mol. Biol 2000;64:65–96. [PubMed: 10697407]
44. Joyce CM, Benkovic SJ. DNA polymerase fidelity: kinetics, structure, and checkpoints. Biochemistry 2004;43:14317–14324. [PubMed: 15533035]
45. Waters ML. Aromatic interactions in model systems. Curr. Opin. Chem. Biol 2002;6:736–741. [PubMed: 12470725]
46. Kool ET. Replication of non-hydrogen bonded bases by DNA polymerases: a mechanism for steric matching. Biopolymers 1998;48:3–17. [PubMed: 9846123]
47. Matray TJ, Kool ET. A specific partner for abasic damage in DNA. Nature 1999;399:704–708. [PubMed: 10385125]
48. Carroll SS, Cowart M, Benkovic SJ. A mutant of DNA polymerase I (Klenow fragment) with reduced fidelity. Biochemistry 1991;30:804–813. [PubMed: 1899034]
49. Bell JB, Eckert KA, Joyce CM, Kunkel TA. Base miscoding and strand misalignment errors by mutator Klenow polymerases with amino acid substitutions at tyrosine 766 in the O helix of the fingers subdomain. J. Biol. Chem 1997;272:7345–7351. [PubMed: 9054433]
50. Lone S, Romano LJ. Mechanistic insights into replication across from bulky DNA adducts: a mutant polymerase I allows an N-acetyl-2-aminofluorene adduct to be accommodated during DNA synthesis. Biochemistry 2003;42:3826–3834. [PubMed: 12667073]

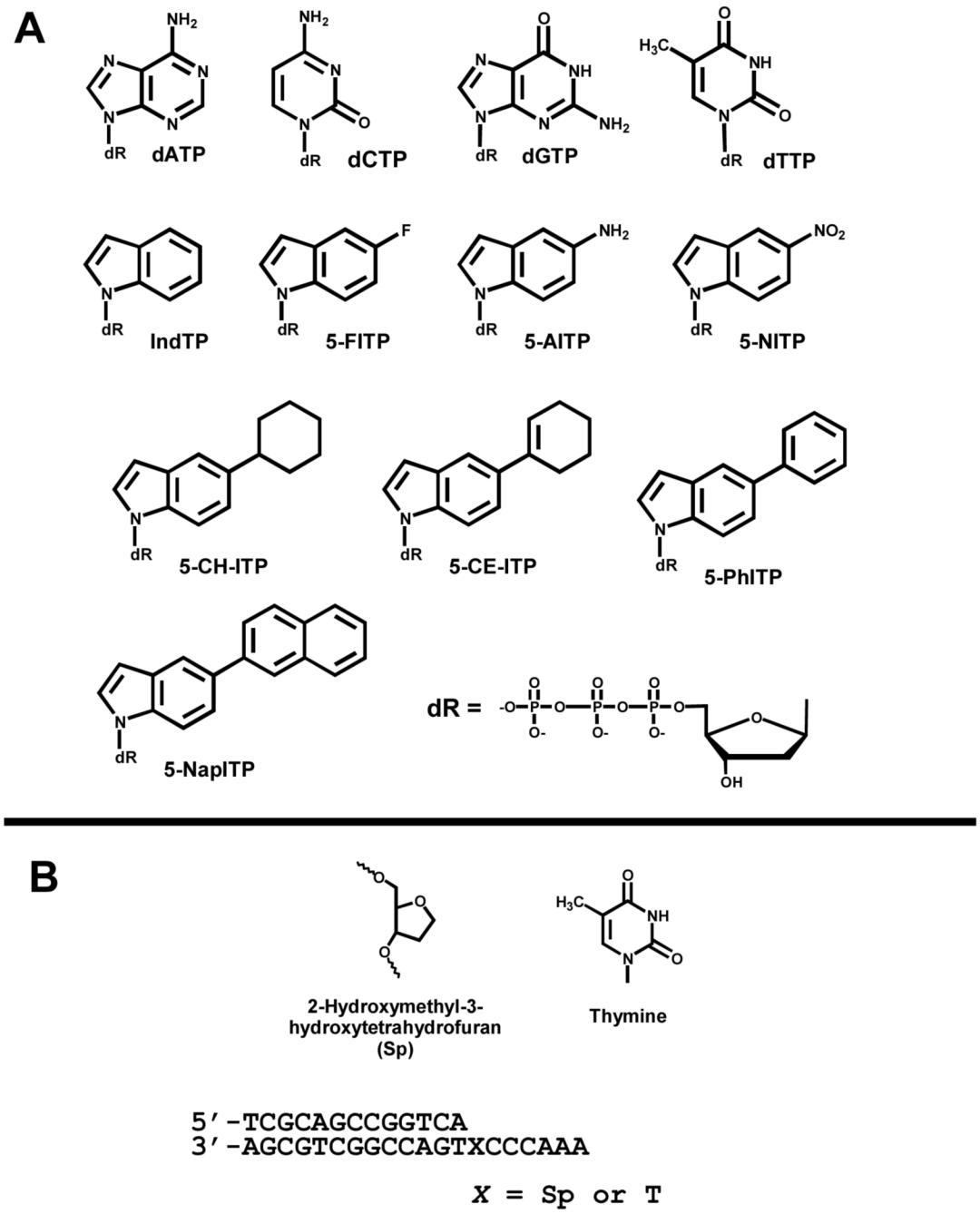

Figure 1.

(A) Structures of 2' deoxynucleoside triphosphates used or referred to in this study are dATP, dCTP, dGTP, dTTP, Ind-TP, 5-FITP, 5-AITP, 5-NITP, 5-PhITP, 5-CE-ITP, 5-CH-ITP, and 5-NapITP. For convenience, dR is used to represent the 2'-deoxyribose 5'-triphosphate portion of the nucleotides. (B) Defined DNA substrates used for kinetic analysis. “X” in the template strand denotes T or the presence of a tetrahydrofuran moiety that mimics an abasic site.

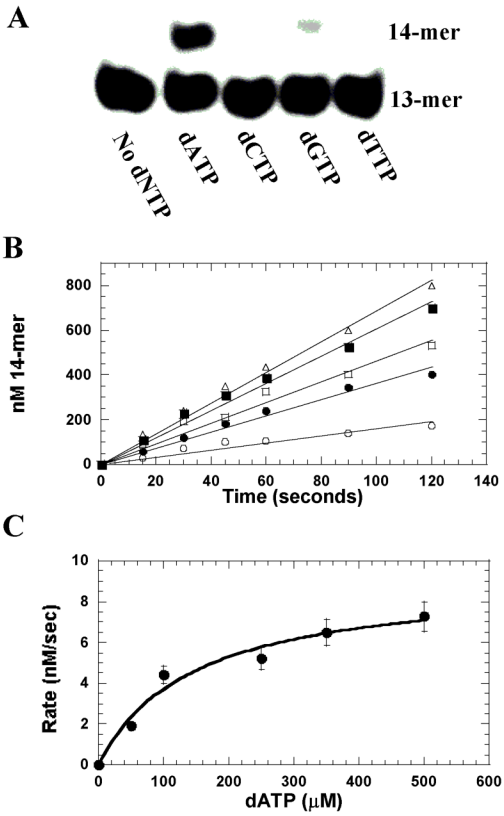

Figure 2.

(A) Representative denaturing gel electrophoresis data for the incorporation of natural nucleotides opposite an abasic site catalyzed by the *E. coli* Klenow fragment. Experiments were performed mixing a preincubated solution of 60 nM Klenow fragment and 1 μM DNA with 100 μM EDTA against 100 μM nucleotide and 10 mM Mg^{2+}. Reactions were quenched at 120 seconds by the addition of 350 mM EDTA. Quenched samples were diluted 1:1 with sequencing gel load buffer and products were analyzed for product formation by denaturing gel electrophoresis. (B) Dependency of the steady-state rate in primer elongation on dATP concentration. The following concentrations of dATP were used: 50 μM (○), 100 μM (●), 250 μM (□), 350 μM (■), and 500 μM (▵). The solid lines represent the fit of each set of data to a straight line. (C) The rates in primer elongation (●) were plotted versus dATP concentration and fit to the Michaelis-Menten equation to determine a K_m of 146 +/- 46 μM and a V_{max} of 9.6 +/- 1.0 nM/sec. The k_{cat} value of 0.8 +/- 0.1 sec^{-1} was obtained by dividing V_{max} by the concentration of polymerase.

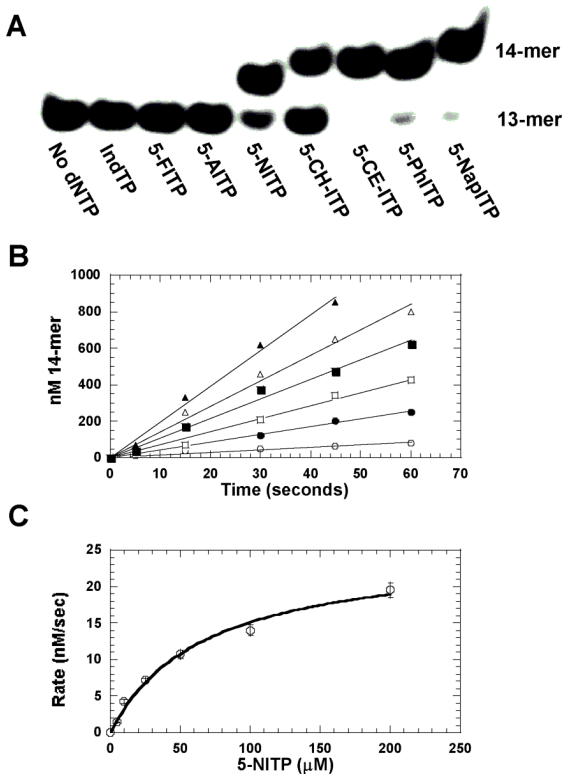

Figure 3.

(A) Representative denaturing gel electrophoresis data for the incorporation of non-natural nucleotides opposite an abasic site catalyzed by the *E. coli* Klenow fragment. Experiments were performed mixing a preincubated solution of 12 nM Klenow fragment and 1 μM DNA with 100 μM EDTA against 100 μM nucleotide and 10 mM Mg^{2+}. Reactions were quenched at 15 seconds by adding 350 mM EDTA. Quenched samples were diluted 1:1 with sequencing gel load buffer and products were analyzed for product formation by denaturing gel electrophoresis. (B) Dependency of the steady-state rate in primer elongation on 5-NITP concentration. The following concentrations of 5-NITP were used: 5 μM (○), 10 μM (●), 25 μM (□), 50 μM (■), 100 μM (▵), and 200 μM (▲). The solid lines represent the fit of each set of data to a linear function to determine rates. (C) The rates in primer elongation (○) were plotted versus 5-NITP concentration and fit to the Michaelis-Menten equation to determine a K_m value of 74 +/- 14 μM and a V_{max} of 28 +/- 2.4 nM/sec. The k_{cat} value of 2.3 +/- 0.2 sec^{-1} was obtained by dividing V_{max} by the concentration of polymerase.

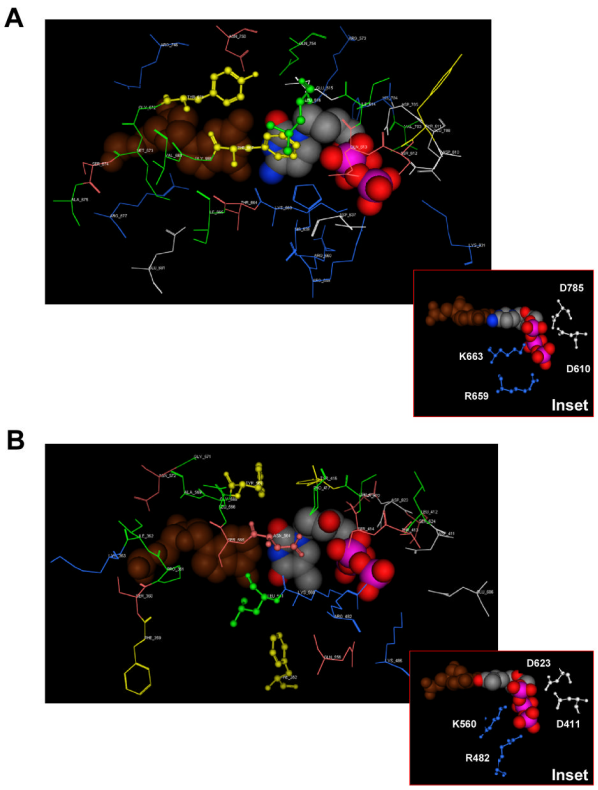

Figure 4.

Comparison of the active sites of the (A) KlenTaq DNA polymerase (PDB ID:3KTQ) and (B) the bacteriophage RB69 DNA polymerase (PDB ID:1IG9) (B). The active site is defined as the amino acids that lie within 6Å from the primer-template junction (shown as a space-filled model). For clarity, these amino acids are color-coded as follows: amino acids that are neutral, hydrophilic, and polar are in orange; amino acids that are positively charged and basic are in blue; amino acids that are negatively charged and acidic are in white; amino acids that are aliphatic and nonpolar are in green; and aromatic amino acids are in yellow. Swiss PDB Viewer 3.7 (www.expasy.org/spdbv) and MOE 2007.09 (www.chemcomp.com) were used to prepare these models. Insets provided in A and B show the arrangement of conserved amino acids that participate in the chemistry of phosphoryl transfer.

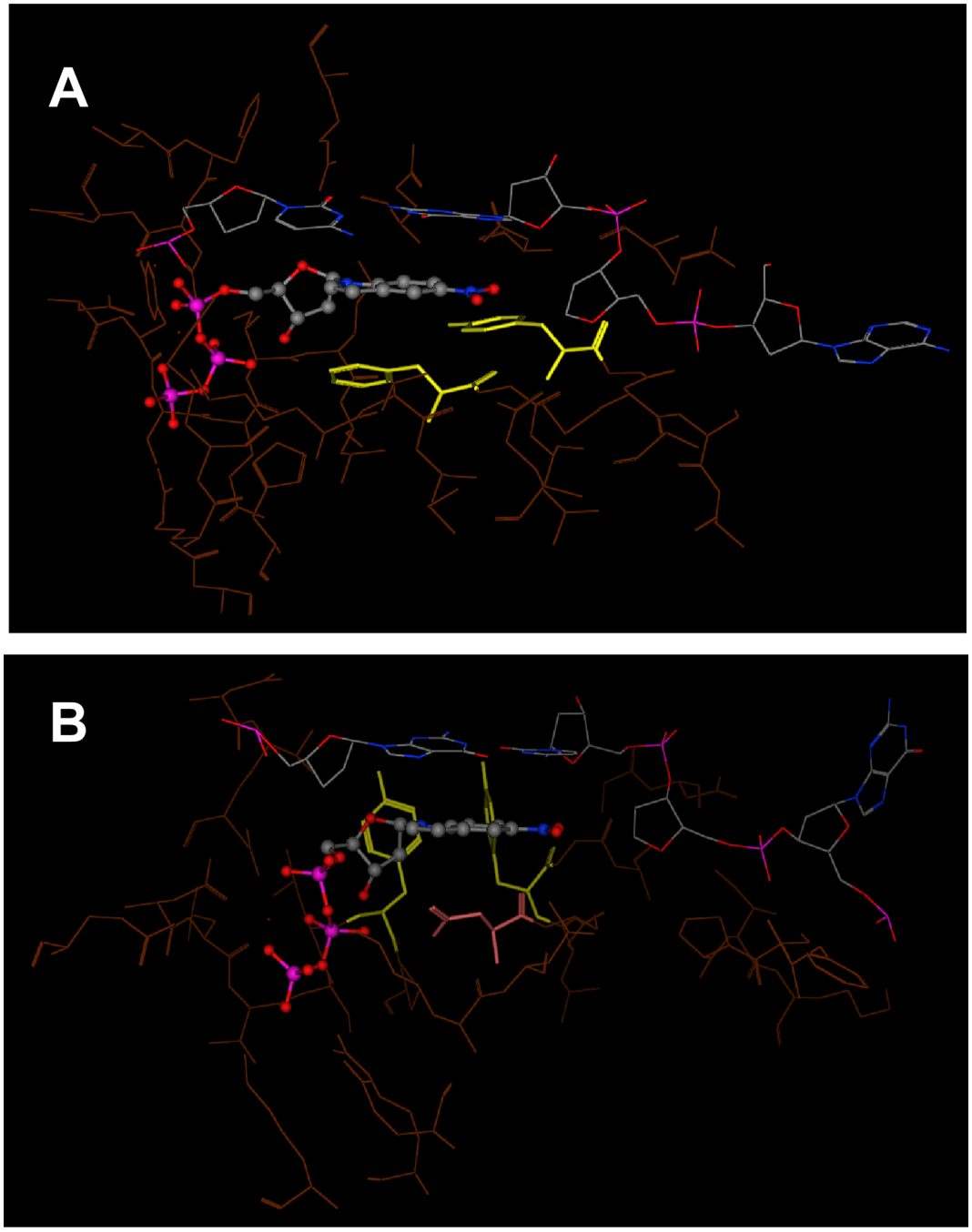

Figure 5.
Comparison of the difference in the orientation of specific residues in the active sites of (A) KlenTaq DNA polymerase with respect to the docked structure of 5-NITP versus (B) the bacteriophage RB69 DNA polymerase with reference to the 5-NITP co-crystallized structure (PDB ID:2OZM).

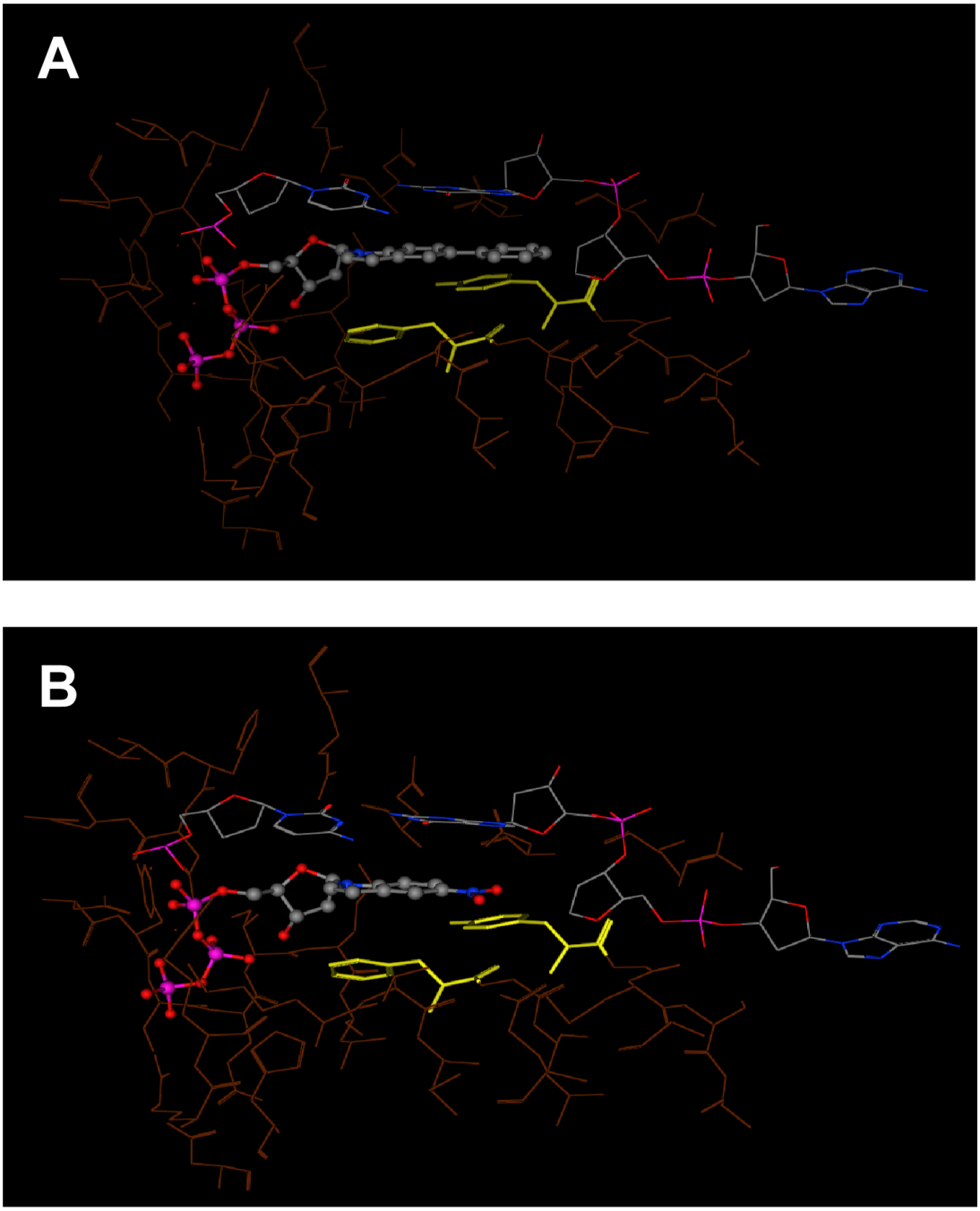

Figure 6.
Comparison of the docked structures of (A) 5-PhITP and (B) 5-NITP in the active site of the KlenTaq DNA polymerase. Both nucleotides are shown in ball and stick representation and in CPK color scheme for clarity. The aromatic amino acids F667 and Y671 are shown in yellow.

Table 1

Summary of kinetic parameters for the incorporation of natural and non-natural nucleotides opposite an abasic site by the *E. coli* Klenow fragment.[a]

Analog	K_m [μM]	k_{cat}(s^{-1})	k_{cat}/Km ($M^{-1}s^{-1}$)	Volume ($Å^3$)[b]	π-Electron Surface Area ($Å^2$) [c]	Dipole Moment (Debye)[d]	Solvation Energy (kcal/mol)[e]
dATP	146 +/- 46	0.8 +/- 0.1	$5.5*10^3$	124.5	145.9	2.57	-18.90
IndTP	ND[f]	ND	ND	132.8	148.1	2.11	-5.45
5-FITP	ND	ND	ND	137.7	148.1	3.57	-4.66
5-AITP	ND	ND	ND	143.2	148.1	1.55	-9.47
5-NITP	74 +/- 14	2.3 +/- 0.2	$3.1*10^4$	154.5	174.0	7.32	-6.92
5-CHITP	34 +/- 9	2.8 +/- 0.3	$8.3*10^4$	228.9	148.1	1.97	-4.23
5-CEITP	6.3 +/- 3.4	2.7 +/- 0.5	$4.3*10^5$	224.2	181.4	2.06	-5.11
5-PhITP	2.8 +/- 0.4	2.5 +/- 0.1	$5.4*10^5$	215.6	225.2	2.66	-6.59
5-NapTP	12 +/- 4	1.3 +/- 0.1	$1.1*10^5$	267.5	274.6	2.73	-7.21

[a] Assays were performed using 12 nM Klenow fragment, 1 μM 13-20-mer containing an abasic site, and variable concentrations of non-natural nucleotide in the presence of 10 mM Mg^{2+}.

[b] Volume (used as an indicator of the relative size of the nucleobase) was calculated using Spartan '04 software.

[c] π-electron surface area refers to the presence of a conjugated functional group at the 5-position of the indolyl-2-deoxyriboside triphosphate and was calculated using Spartan '04 software.

[d] Dipole moments (debye) refer to and were calculated using Spartan '04 software.

[e] Solvation energies for each nucleobase were calculated using Spartan '04 software.

[f] Not determined as nucleotide incorporation was not detected even at the highest concentration of nucleotide tested (500 μM).

Table 2

Kinetic parameters for the incorporation of non-natural nucleotides opposite thymine catalyzed by the Klenow fragment from *E. coli.*[a]

Analog	K_m [μM]	k_{cat} (s^{-1})	k_{cat}/K_m (M^{-1} sec^{-1})
DATP	5+/-1[b]	50 +/- 5[b]	$1*10^7$
IndTP	ND[c]	ND	ND
5-FITP	32 +/- 7	0.014 +/- 0.001	440 +/- 50
5-AITP	ND	ND	ND
5-NITP	180 +/- 20	0.032 +/- 0.002	180 +/- 35
5-PhITP	58 +/- 15	0.025 +/- 0.002	430 +/- 40
5-CE-ITP	ND	ND	ND
5-CH-ITP	ND	ND	ND
5-NapTP	23 +/- 7	0.026 +/- 0.004	1,130 +/- 150

[a] Assays were performed using 60 nM Klenow fragment, 1 μM 13-20-mer containing a thymine, and variable concentrations of non-natural nucleotide in the presence of 10 mM Mg^{2+}.

[b] Kinetic parameters for the incorporation of dATP are taken from Kuchta *et al.* (34) and are provided for comparison.

[c] Not determined as nucleotide incorporation was not detected even at the highest concentration of nucleotide tested (500 μM).

Table 3

Comparison of kinetic parameters for the incorporation of non-natural nucleotides opposite an abasic site catalyzed by the *E. coli* Klenow fragment versus the bacteriophage T4 DNA polymerase.[a]

	Klenow Fragment		Bacteriophage T4 DNA Polymerase	
Analog	**K_m [μM]**	**k_{cat} (s^{-1})**	**K_d [μM]**	**k_{pol} (s^{-1})**
dATP	146 +/- 46	0.8 +/- 0.1	35 +/- 5	0.15 +/- 0.01[c]
IndTP	ND	ND[b]	145 +/- 10[d]	0.28 +/- 0.07[d]
5-FITP	ND	ND	152 +/- 41[e]	0.30 +/- 0.03[e]
5-AITP	ND	ND	255 +/- 43[e]	0.17 +/- 0.01[e]
5-NITP	74 +/- 14	2.3 +/- 0.2	18 +/- 3[f]	126 +/- 7[f]
5-CH-ITP	34 +/- 9	2.8 +/- 0.3	44 +/- 14[g]	0.70 +/- 0.13[g]
5-CE-ITP	6.3 +/- 3.4	2.7 +/- 0.5	5.1 +/-1.7[g]	25 +/- 2[g]
5-PhITP	2.8 +/- 0.4	2.5 +/- 0.1	14 +/- 3[e]	53 +/- 4[e]
5-NapTP	12 +/- 4	1.3 +/- 0.1	10 +/- 5[h]	27 +/- 4[h]

[a] Assays were performed using 60 nM Klenow fragment, 1 μM 13-20T-mer, and variable concentrations of non-natural nucleotide in the presence of 10 mM Mg^{2+}.

[b] Not determined as incorporation was not detected at the highest concentration of nucleotide tested (500 μM).

[c] Values taken from Berdis (25).

[d] Values taken from Zhang *et al.* (17).

[e] Values taken from Zhang *et al.* (18).

[f] Values taken from Reineks and Berdis (16).

[g] Values taken from Zhang *et al.* (19).

[h] Values taken from Zhang *et al.* (20).